White light emission from Er, Pr co-doped AlN films

Xiang Li (李 祥)[1], Xiaodan Wang (王晓丹)[1,*], Hai Ma (马 海)[1], Feifei Chen (陈飞飞)[1], and Xionghui Zeng (曾雄辉)[2,]**

[1]*Jiangsu Key Laboratory of Micro and Nano Heat Fluid Flow Technology and Energy Application, School of Mathematics and Physics, Suzhou University of Science and Technology, Suzhou 215009, China*

[2]*Suzhou Institute of Nano-Tech and Nano-Bionics, Chinese Academy of Sciences, Suzhou 215123, China*

**Corresponding author: xdwang0416@163.com; **corresponding author: xhzeng2007@sinano.ac.cn*

Received May 7, 2019; accepted July 5, 2019; posted online September 10, 2019

In this work, Er-doped aluminum nitride (AlN), Pr-doped AlN, and Er, Pr co-doped AlN thin films were prepared by ion implantation. After annealing, the luminescence properties were investigated by cathodoluminescence. Some new and interesting phenomena were observed. The peak at 480 nm was observed only for Er-doped AlN. However, for Er, Pr co-doped AlN, it disappeared. At the same time, a new peak at 494 nm was observed, although it was not observed for Er-doped AlN or Pr-doped AlN before. Therefore, the energy transfer mechanism between Er^{3+} and Pr^{3+} in AlN thin films was investigated in detail. Through optimizing the dose ratio of Er^{3+} with respect to Pr^{3+}, white light emission with an International Commission on Illumination chromaticity coordinate (0.332, 0.332) was obtained. This work may provide a new strategy for realizing white light emission based on nitride semiconductors.

OCIS codes: 160.4760, 160.5690, 160.6000.
doi: 10.3788/COL201917.111602.

Aluminum nitride (AlN) belongs to an atomic crystal with strong chemical bonds, so it is chemically inert in most environments. Meanwhile, AlN has potential applications in the optoelectronic field due to its direct band gap. Because of its large band gap (−6.2 eV), AlN is transparent in the wavelength range from the ultraviolet (UV) to the infrared (IR)[1–3]. Owing to the above properties, AlN is a suitable host for rare earth (RE) ions.

For the past decades, great progress has been made in the field of RE-doped GaN materials[4–9]. However, the investigations of RE-doped AlN are still in the primary stage. In fact, AlN belongs to the $P6_3mc$ space group and has the same crystal structure as GaN. The RE ions substitute Al ions sites with C_{3v} crystal symmetry during crystal growth[1]. For RE ions, according to Laporte selective rule, the transitions of the 4f shell accounting for emission are forbidden, but the selections are relaxed due to the mixture between odd state and couple state caused by the impact of crystal fields[10].

Efforts on Er-doped AlN materials have been under way[1,11,12]. Kallel *et al.* have grown Er-doped AlN thin film by using molecular beam epitaxy (MBE) and studied the spectral properties. The main emission peak is blue light; the authors also calculated the energy levels of Er by the crystal field theory. The results of the experiments are consistent with the calculation, which demonstrates that Er ions substitute the lattice sites of Al ions in AlN[1]. For the Pr-doped AlN materials, some research works have been carried out[13,14]. The optical properties of Pr-implanted AlN films grown by MBE have been reported by Lozykowski *et al.* Green light emission was observed from the films[13].

Based on previous works mentioned above, if Er ions and Pr ions are co-doped into AlN film, the film may simultaneously emit green light and blue light under excitation and realize white light emission. However, until now, there have been no such reports. On the other hand, there are few reports about RE co-doped AlN or GaN, such as Er, Tm co-doped AlN[15], Pr, Tm co-doped GaN[16], Pr, Er, Tm co-doped GaN[17], and Eu, Pr co-doped GaN and AlN[18]. In this Letter, Er and Pr co-doped AlN films were prepared through ion implantation. The luminescence properties were measured by cathodoluminescence (CL) spectroscopy. The energy transfer mechanism between Er^{3+} and Pr^{3+} in AlN thin films was investigated in detail. Through optimizing the dose ratio of Er^{3+} with respect to Pr^{3+}, for the first time, to the best of our knowledge, white light emission with Commission Internationale De L′E′clairage (CIE) chromaticity coordinate (0.332, 0.332) was obtained from Er and Pr co-doped AlN films.

The 2 μm thick AlN films were grown by hydride vapor phase epitaxy (HVPE) on (0001) sapphire substrates. The growth details were reported elsewhere[19]. Er, Pr ions were doped into AlN films through ion implantation with the energy of 200 keV. The implanting ion beam was inclined about 10° with respect to the normal of the AlN films for reducing the channeling effect. In the Er-doped AlN, the implantation dose is 1×10^{14} at/cm^2 (atoms per square centimeter) and 5×10^{14} at/cm^2, respectively. In the Pr-doped AlN, the implantation dose is 1×10^{14} at/cm^2, 5×10^{14} at/cm^2, and 1×10^{15} at/cm^2, respectively. In the Er, Pr co-doped AlN samples, the dose of Er^{3+} ions is kept at 1×10^{14} at/cm^2, and the dose of Pr^{3+} is 1×10^{14} at/cm^2, 5×10^{14} at/cm^2, and 1×10^{15} at/cm^2, respectively. All of the implanted samples were annealed at 1050°C under a flow of N_2 at one atmospheric pressure. Luminescence properties were measured by a MonoCL3+ CL spectrometer installed on a

Quanta400FEG field emission scanning electron microscope (SEM). The accelerating voltage is 5 kV, the grating is 1200 l/mm, and the slit width is 1 mm. All measurements were carried out at room temperature.

In our previous work, the luminescence properties of Er-doped AlN have been reported[15]. The CIE chromaticity coordinate of emission light is (0.284, 0.272). Obviously, it is far from the standard white light coordinate (0.333, 0.333). Figure 1 shows the luminescence spectrum of Pr^{3+}-implanted AlN with a dose of 5×10^{14} at/cm^2 after annealing at 1050°C. The luminescence peaks at 528, 657, and 675 nm belong to $^3P_1 \rightarrow {}^3H_5$, $^3P_0 \rightarrow {}^3F_2$, and $^3P_0 \rightarrow {}^3F_3$ transitions of Pr^{3+}, respectively. The broad peaks at 378 and 480 nm are related to oxygen impurity and Al vacancy, respectively[15]. The CIE chromaticity coordinate of emission light is (0.300, 0.287).

As shown in the inset of Fig. 1, the luminescence intensity of the peak at 528 nm is the highest when the implantation dose is 5×10^{14} at/cm^2. The non-radiative recombination rate is determined from the distance between Pr^{3+} ions and defects[16]. When the implantation dose is as low as 1×10^{14} at/cm^2, the distance between Pr^{3+} ions and defects is also large, and then the non-radiative recombination rate is low. However, due to the low dose of Pr^{3+}, the luminescence intensity is not the highest in this work. On the other hand, if the implantation dose is too high, such as 1×10^{15} at/cm^2, then the non-radiative recombination rate is too high, as a result, the luminescence intensity decreases, as shown in the inset of Fig. 1. In this work, 5×10^{14} at/cm^2 may be the optimal dose for Pr^{3+}-implanted AlN films.

Figure 2(a) shows the CL spectra of three Er^{3+} and Pr^{3+} co-implanted AlN films with different dose ratios of Er^{3+} with respect to Pr^{3+}. For all three samples, a peak at 494 nm was observed and attributed to the transition of $^3P_0 \rightarrow {}^3H_4$ of Pr^{3+}[20], which was not observed in the Pr^{3+}-implanted AlN sample. On the other hand, with the increase of the Pr dose in Er, Pr co-implanted AlN, the luminescence peak at 480 nm, belonging to the transition of $^4F_{7/2} \rightarrow {}^4I_{15/2}$ of Er^{3+}, became weaker and weaker. Therefore, the energy transfer process labeled

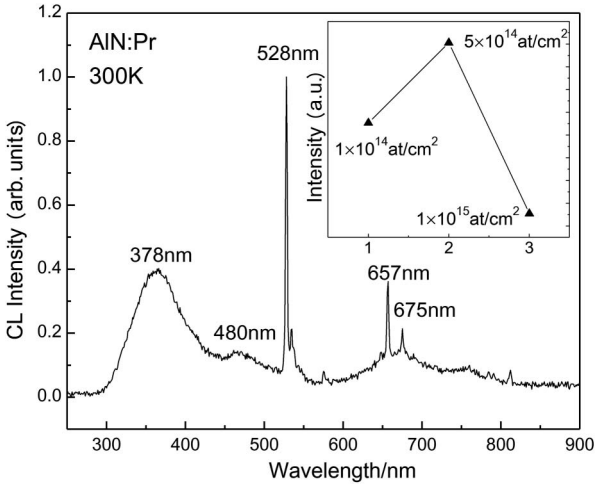

Fig. 1. CL spectrum of Pr^{3+}-implanted AlN with a dose of 5×10^{14} at/cm^2 after annealing at 1050°C. Inset is the dependence of the intensity of the 528 nm luminescence peak on the implantation dose.

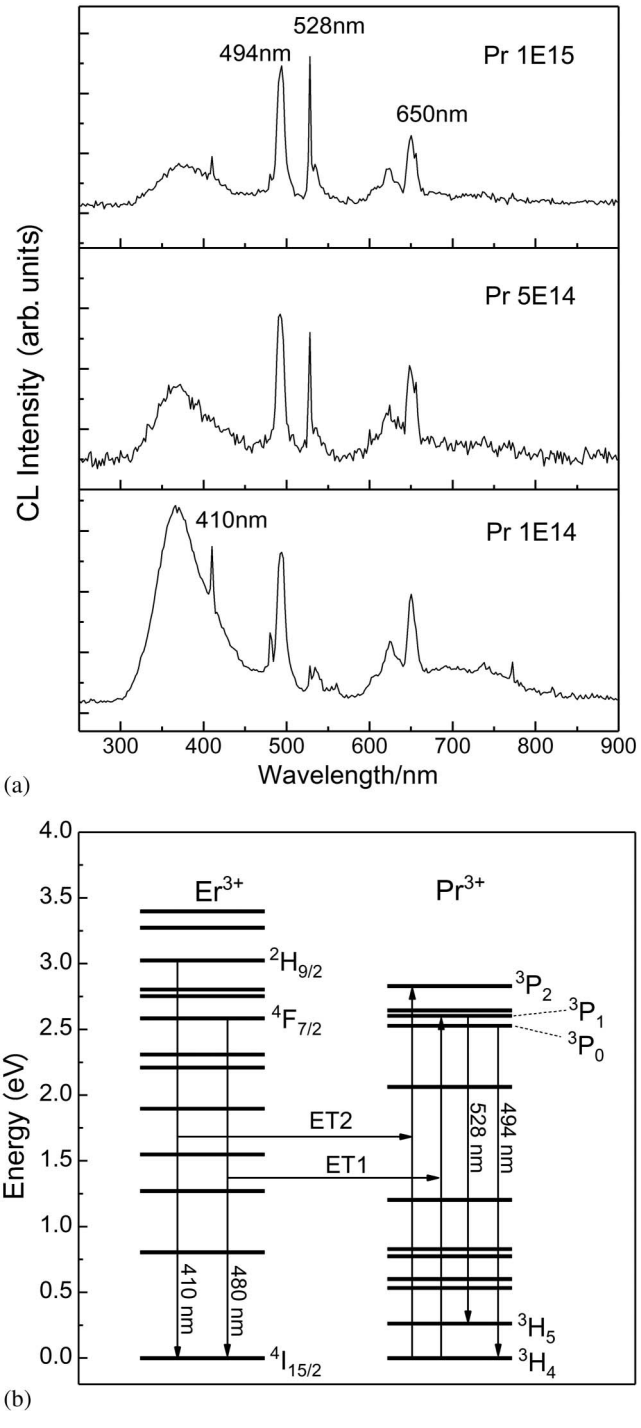

Fig. 2. CL spectra and energy transfer model of Er^{3+} and Pr^{3+} co-implanted AlN thin films with the different dose ratios of Pr^{3+} with respect to Er^{3+}, where the dose of Er is kept as 1×10^{14} at/cm^2. (a) CL spectra of Er^{3+} and Pr^{3+} co-implanted AlN. (b) Energy transfer model between Er^{3+} and Pr^{3+}.

as ET1 in Fig. 2(b) between Er^{3+} and Pr^{3+} is possible. Due to nearly equivalent energy gap between $^3P_1 \rightarrow {}^3H_4$ of Pr^{3+} and $^4F_{7/2} \rightarrow {}^4I_{15/2}$ of Er^{3+}, resonant energy transfer is possible. The electrons on the excited state $^4F_{7/2}$ are de-excited to the ground state $^4I_{15/2}$ through non-radiative relaxation, and the energy is transferred to Pr^{3+} through resonant energy transfer. The electrons on the ground state $^3H_4$ of Pr^{3+} are excited to the excited state $^3P_1$ and relaxed to the lower excited state $^3P_0$; then, the transition of $^3P0 \rightarrow {}^3H_4$ corresponding to the 494 nm luminescence peak is observed, and the transition of $^4F_{7/2} \rightarrow {}^4I_{15/2}$ of Er^{3+} corresponding to the 480 nm luminescence peak nearly disappears.

The efficiency of the energy transfer is mainly determined from the average distance between RE ions[13]. In this work, the average distance is related to the implantation dose of Pr^{3+} and Er^{3+}. When both of the doses of Er^{3+} and Pr^{3+} are 1×10^{14} at/cm^2, the average distance between Er^{3+} and Pr^{3+} is relatively large. Although the new luminescence peak at 494 nm of Pr^{3+} appears, the luminescence peak at 480 nm of Er^{3+} can still be observed. With the increase of dose of Pr^{3+}, the average distance between Er^{3+} and Pr^{3+} decreases, which is favorable for the energy transfer process. Therefore, when the dose of Pr^{3+} is 5×10^{14} at/cm^2, the luminescence peak at 480 nm nearly disappears, and the intensity of luminescence peak at 528 nm increases.

Two more interesting phenomena were also observed. In Fig. 1, the peak luminescence intensity at 528 nm has maximum and minimum values when the Pr^{3+} implantation dose is 5×10^{14} and 1×10^{15} at/cm^2, respectively. However, in Fig. 2, peak luminescence intensity at 528 nm is highest when the Pr^{3+} implantation dose is 1×10^{15} at/cm^2. In addition, according to our previous work[15], compared with Er-doped AlN, the peak luminescence intensity at 410 nm belonging to the $^2H_{9/2}$ to $^4I_{15/2}$ transition of Er^{3+} is obviously decreased in Er, Pr co-implanted AlN. The energy difference between $^2H_{9/2}$ to $^4I_{15/2}$ of Er^{3+} and $^3P_2$ to $^3H_4$ of Pr^{3+} is only about 150 meV. Considering the assistance of phonons in the AlN lattice[21], the energy transfer process labeled as ET2 in Fig. 2(b) is possible. Then, the non-radiation transition from $^3P_2$ to $^3P_1$ of Pr^{3+} is expected. Therefore, for Er, Pr co-implanted AlN, the peak luminescence intensity at 410 nm is decreased obviously, and, with the Pr dose increase, the peak luminescence intensity at 528 nm is enhanced significantly. Here, we also noticed that the intensity at 410 nm is not decreased monotonously. This phenomenon needs to be investigated further in the near future.

We also calculate the CIE chromaticity coordinate of emission light of Er, Pr co-implanted AlN films. The results are listed in Table 1.

The CIE chromaticity coordinate of standard white light is (0.333, 0.333). Therefore, when the dose of Er^{3+} and Pr^{3+} in AlN films is 1×10^{14} and 5×10^{14} at/cm^2, respectively, the emission light is nearly white light. Figure 3 is the CIE chromaticity diagram.

Table 1. The CIE Chromaticity Coordinate of Er, Pr Co-implanted AlN Films

Er^{3+}/Pr^{3+}(at/cm^2)	CIE X	CIE Y
$1 \times 10^{14}/1 \times 10^{14}$	0.323	0.312
$1 \times 10^{14}/5 \times 10^{14}$	0.332	0.332
$1 \times 10^{14}/1 \times 10^{15}$	0.329	0.335

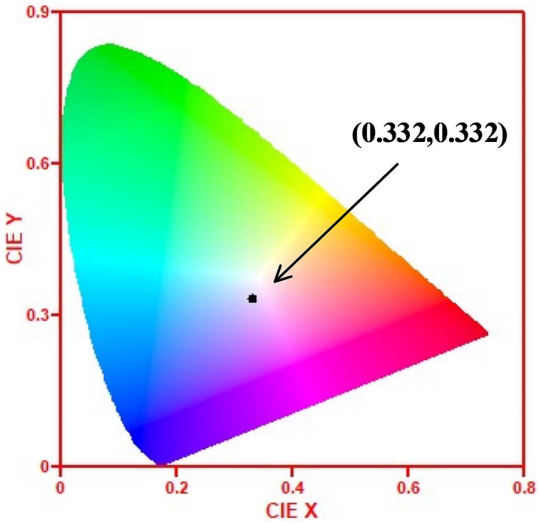

Fig. 3. CIE chromaticity diagram of Er^{3+}, Pr^{3+} co-doped AlN film. The doses of Er^{3+} and Pr^{3+} in AlN films are 1×10^{14} and 5×10^{14} at/cm^2.

In conclusion, through co-implanting Er, Pr in AlN films, a new luminescence peak at 494 nm was observed and attributed to the transition of $^3P0 \rightarrow {}^3H_4$ of Pr^{3+}, which was not observed in Pr-implanted AlN films. At the same time, the luminescence peak at 480 nm belonging to the transition of $^4F_{7/2} \rightarrow {}^4I_{15/2}$ of Er^{3+} became weaker and weaker with the increase of the Pr dose. We concluded that there is an energy transfer between Er^{3+} and Pr^{3+} ions. When the dose of Er^{3+} and Pr^{3+} in AlN films is 1×10^{14} and 5×10^{14} at/cm^2, we obtained an ideal CIE chromaticity coordinate (0.332, 0.332). This work demonstrated a way for realizing white light emission in AlN films through co-doping RE ions.

This work was supported by the National Natural Science Foundation of China (Nos. 61306004 and 51002179), the Program of Suzhou Key Laboratory for Low Dimensional Optoelectronic Materials and Devices (No. SZS201611), the Jiangsu Key Disciplines of 13th Five-Year Plan (No. 20168765), and the Graduate Research and Practice Innovation Project of USTS (Nos. SKCX18_Y11 and SKCX17_034).

References

1. T. Kallel, T. Koubaa, M. Dammak, J. Wang, and W. M. Jadwisiencazk, J. Luminesc. **134**, 893 (2013).

2. G. Yan, G. Chen, F. Qiu, and Y. Zhao, Acta. Photon. Sin. **35**, 221 (2006).
3. C. Li, X. Ren, H. Wu, R. Zheng, J. Zhao, D. Ouyang, C. Du, P. Yan, and S. Ruan, Chin. Opt. Lett. **16**, 043201 (2018).
4. Y. Mo, X. Wang, X. Zeng, W. Gao, J. Wang, and K. Xu, J. Synth. Cryst. **44**, 1569 (2015).
5. A. Nishikawa, T. Kawasaki, N. Furukawa, Y. Terai, and Y. Fujiwara, Appl. Phys. Express **2**, 071004 (2009).
6. Y. Mo, X. Wang, M. Yang, X. Zeng, J. Wang, and K. Xu, Phys. Status Solidi B Basic Solid State Phys. **253**, 515 (2016).
7. H. Huang, D. Yan, G. Wang, F. Xie, G. Yang, S. Xiao, and X. Gu, Chin. Opt. Lett. **12**, 092301 (2014).
8. J. S. Kang, J. A. Yoon, S. I. Yoo, J. W. Kim, B. M. Lee, H. H. Yu, C. B. Moon, and W. Y. Kim, Chin. Opt. Lett. **13**, 032301 (2015).
9. X. Wang, Y. Mo, X. Zeng, H. Mao, J. Wang, and K. Xu, Chin. Opt. Lett. **14**, 051602 (2016).
10. F. Qi, F. Huang, T. Wang, R. Lei, J. Zhang, S. Xu, and L. Zhang, Chin. Opt. Lett. **15**, 051604 (2017).
11. H. Rinnert, S. S. Hussain, V. Brien, J. Legrand, and P. Pigeat, J. Luminesc. **132**, 2367 (2012).
12. M. Maabool, I. Ahmad, G. Ali, and K. Maaz, Opt. Mater. **46**, 601 (2015).
13. H. J. Lozykowski, W. M. Jadwisienczak, A. Bensaoula, and O. Monteiro, Microelectron. J. **36**, 453 (2005).
14. M. Fialho, S. Magalhaes, L. C. Alves, C. Marques, R. Maalej, T. Monteiro, K. Lorenz, and E. Alves, Nucl. Instrum. Methods Phys. Res B. **273**, 149 (2012).
15. X. Wang, M. Yang, X. Zeng, Y. Mo, J. Zhang, J. Wang, and K. Xu, J. Alloy Compd. **726**, 209 (2017).
16. X. Wang, Y. Mo, M. Yang, X. Zeng, J. Wang, and K. Xu, Opt. Mater. Express. **6**, 1692 (2016).
17. X. Wang, Y. Mo, X. Zeng, J. Wang, and K. Xu, Mater. Chem. Phys. **199**, 567 (2017).
18. J. Rodrigues, S. M. C. Miranda, N. F. Santos, A. J. Neves, E. Alves, K. Lorenz, and T. Monteiro, Mater. Chem. Phys. **134**, 716 (2012).
19. M. Sun, J. Zhang, J. Huang, J. Wang, and K. Xu, J. Cryst. Growth **436**, 62 (2016).
20. M. Maqbool, I. Ahmad, H. H. Richardson, and M. E. Kordesch, Appl. Phys. Lett. **91**, 193511 (2007).
21. M. Kaneko, T. Kimoto, and J. Suda, AIP Adv. **7**, 015105 (2017).